

Spiral phase and phase separation of the double exchange model in the large-S limit

Lan Yin*

School of Physics, Peking University, Beijing 100871, P. R. China

(Dated: November 14, 2018)

The phase diagram of the double exchange model is studied in the large-S limit at zero temperature in two and three dimensions. We find that the spiral state has lower energy than the canted antiferromagnetic state in the region between the antiferromagnetic phase and the ferromagnetic phase. At small doping, the spiral phase is unstable against phase separation due to its negative compressibility. When the Hund coupling is small, the system separates into spiral regions and antiferromagnetic regions. When the Hund coupling is large, the spiral phase disappears completely and the system separates into ferromagnetic regions and antiferromagnetic regions.

The colossal magnetoresistance effect (CMR) was discovered in hole-doped manganese oxides such as $\text{La}_{1-x}\text{Sr}_x\text{MnO}_3$ and $\text{La}_{1-x}\text{Ca}_x\text{MnO}_3$ [1]. Various experiments have revealed that these materials have very rich phase diagrams [2]. In these materials, the three t_{2g} electrons form a localized $S = 3/2$ Kondo spin at each manganese site and e_g electrons form a conduction band. The degeneracy of the two e_g orbitals is lifted by Jahn-Teller effect and only one of the orbitals is close to the fermi energy. The e_g spins interact with t_{2g} spins through Hund coupling. The single orbital double exchange (DE) model [3] is the simplest description of this system. There are other important factors in this system, such as Jahn-Teller phonons, exchange interaction between the Kondo spins, and Columb interaction. It is important to study the DE model and identify its role in the CMR systems.

The ferromagnetic phase of the DE model have been studied in the past [3, 4]. De Gennes studied the DE model with the exchange interaction and found that the system goes into a canted antiferromagnetic (CAF) phase near half filling [5]. However numerical studies [6] discovered phase separation in the simple DE model near half filling in one, two and infinite dimensions. There is some evidence that it occurs in three dimensions as well. In addition, an incommensurate phase was found when Hund coupling is relatively small. Phase separation was also found in DE models with exchange interaction and with Jahn-Teller phonons [7].

Some theoretical studies [8, 9, 10, 11, 12] have been focused on phase separation in the DE model. Phase separation was also found in the limit of infinite Hund coupling near Curie temperature, but absent in zero temperature [8]. The DE model was mapped onto a $t - J$ model in Ref. [9] where phase separation was found not only near half filling [13], but also near zero filling. The stability of canted antiferromagnetic state was examined in Ref. [10] and phase separation was found in certain parameter regions, but it is unclear that without exchange interaction whether the phase separation exists or not. In Ref. [11] and Ref. [12], phase separation was found in the DE model within the dynamic mean field approximation.

In this paper, we study the zero-temperature phase diagram of the simple DE model in the large-S limit in cubic and square lattices. At zero doping, the system is in an antiferromagnetic phase. At a high level of doping, the system goes into a ferromagnetic phase. We find that in the region between the antiferromagnetic phase and the ferromagnetic phase, the spiral state has the lower energy than the CAF state. However, the spiral state is always unstable near half filling and subject to phase separation. When the ratio of Hund coupling to hopping energy is below certain critical value, the separation is between the antiferromagnetic phase and the spiral phase. Above this ratio, the spiral phase is always unstable and the system always separates into antiferromagnetic phase and ferromagnetic phase. There is one qualitative difference between 2D and 3D systems. In 3D, in the limit of zero Hund coupling, the transition between the ferromagnetic phase and the spiral phase occurs at hole density around 0.55; in the same limit, the critical density approaches 1 in 2D.

The Hamiltonian of the DE model is given by

$$\mathcal{H} = -t \sum_{\langle ij \rangle, \sigma} c_{i\sigma}^\dagger c_{j\sigma} - J \sum_i \mathbf{S}_i \cdot \mathbf{s}_i, \quad (1)$$

where \mathbf{s}_i is the electron spin with total spin 1/2 and \mathbf{S}_i is the Kondo spin with total spin S . In this paper, we consider the Kondo spins as classical spins which is exact in the large- S limit. The quantum correction to this approximation is smaller by a factor of $1/S$ and vanishes in the large- S limit. The classical spin approximation is also equivalent to trial wave-functions with static spin configuration. Thus it can provide an upper bound for ground state energy.

*Electronic address: yinlan@pku.edu.cn; Former address: Department of Physics, University of Washington, Seattle, WA 98195-1560

We consider the possible phases of the system. For convenience, we use the electron operators f_i and h_i which have spins parallel and opposite to the Kondo spin,

$$\begin{aligned} c_{i\uparrow} &= \cos(\theta_i/2)e^{i\alpha_i}f_i + \sin(\theta_i/2)e^{-i(\alpha_i+\phi_i)}h_i, \\ c_{i\downarrow} &= -\cos(\theta_i/2)e^{-i\alpha_i}h_i + \sin(\theta_i/2)e^{i(\alpha_i+\phi_i)}f_i, \end{aligned}$$

where α_i is an arbitrary phase factor, and θ_i and ϕ_i are the azimuth and polar angles of \mathbf{S}_i . For the Kondo spins, it is convenient to use the Schwinger-boson representation [16], $b_{i\uparrow} = \sqrt{2S}\cos(\theta_i/2)e^{i\alpha_i}$ and $b_{i\downarrow} = \sqrt{2S}\sin(\theta_i/2)e^{i(\phi_i+\alpha_i)}$ with the constraint $\sum_{\sigma} b_{i\sigma}^* b_{i\sigma} = 2S$. In the classical spin approximation, the Schwinger-boson operators are just complex numbers. In terms of the new fermion operators and the Schwinger-boson operators, the Hamiltonian is given by

$$\begin{aligned} \mathcal{H} &= -\frac{t}{2S} \sum_{\langle ij \rangle} \left[(f_i^\dagger f_j + h_j^\dagger h_i) \sum_{\sigma} b_{i\sigma}^* b_{j\sigma} + (f_i^\dagger h_j (b_{i\uparrow}^* b_{j\downarrow}^* - b_{j\uparrow}^* b_{i\downarrow}^*) + h.c.) \right] \\ &\quad - \frac{JS}{2} \sum_i (f_i^\dagger f_i - h_i^\dagger h_i). \end{aligned} \quad (2)$$

In the ferromagnetic phase, all the Kondo spins are aligned in the same direction, and the electron hopping amplitude is diagonal and at maximum, $\sum_{\sigma} b_{i\sigma}^* b_{j\sigma} = 2S$ and $b_{i\uparrow} b_{j\downarrow} - b_{j\uparrow} b_{i\downarrow} = 0$. The h - and f -fermions are free particles with the dispersion given by $E_{\mathbf{k}} = \epsilon_{\mathbf{k}} \pm \frac{1}{2}JS$, where $\epsilon_{\mathbf{k}} = -2t \sum_{\alpha=1}^d \cos k_{\alpha}a$, a is the lattice spacing and d is the dimensionality. When the electron bandwidth $4dt$ is bigger than the Hund energy splitting JS , for less than half filling, only the lower band is occupied and this fully-magnetized state is an exact eigenstate of the Hamiltonian. When $JS < 4dt$ and sufficiently close to half filling, both bands become occupied and the ferromagnetic state is no longer an exact eigenstate but an approximation. It is straight forward to go beyond classical spin approximation and show that the spin fluctuations are essentially described by spin waves with quadratic dispersion [3, 4], much like in a typical Heisenberg ferromagnet. At zero temperature, the spin waves are frozen out and do not provide any significant change to the classical spin configuration.

We have also considered the possibility of a totally disordered state. However, in the classical spin approximation it is insufficient to consider such a state. We use a mean-field Schwinger-boson formalism [16] instead. But we found that the saddle point of the disordered state does not exist at zero temperature for any positive integer or half-integer Kondo spin in dimensions higher than or equal to two.

Exactly at half filling, the system is in an antiferromagnetic phase. For simplicity, we choose the Kondo spins aligning in the x -direction, $b_{i\uparrow} = \sqrt{S}e^{-i\mathbf{Q}\cdot\mathbf{R}_i}$ and $b_{i\downarrow} = \sqrt{S}e^{i\mathbf{Q}\cdot\mathbf{R}_i}$, where $\mathbf{Q} = (\frac{\pi}{2a}, \frac{\pi}{2a}, \frac{\pi}{2a})$. The hopping matrix becomes completely off-diagonal, $\sum_{\sigma} b_{i\sigma}^* b_{j\sigma} = 0$ and $b_{i\uparrow} b_{j\downarrow} - b_{j\uparrow} b_{i\downarrow} = -2iS \sin(\mathbf{Q} \cdot (\mathbf{R}_i - \mathbf{R}_j))$. The fermions form two bands with dispersion given by $E_{\mathbf{k}} = \pm \sqrt{\frac{J^2 S^2}{4} + \epsilon'_{\mathbf{k}}{}^2}$, where $\epsilon'_{\mathbf{k}} = -2t \sum_{\alpha} \sin k_{\alpha}a$. The free-fermion operators are linear combinations of the f - and h -operators. At half filling, only the lower band is occupied.

In comparison, when $JS > 4dt$, the lower band of the ferromagnetic state is completely filled and the total hopping energy is zero at half filling. It is clear that the antiferromagnetic phase has lower energy in this case. When $JS < 4dt$, the total energy difference between these two states is given by

$$\Delta E = \int_{-\frac{1}{2}JS}^{\frac{1}{2}JS} \left(\sqrt{\left(\frac{1}{2}JS\right)^2 + \epsilon^2} - \frac{1}{2}JS \right) N(\epsilon) d\epsilon + \int_{\frac{1}{2}JS}^{2dt} 2 \left(\sqrt{\left(\frac{1}{2}JS\right)^2 + \epsilon^2} - \epsilon \right) N(\epsilon) d\epsilon, \quad (3)$$

where $N(\epsilon) \equiv \sum_{\mathbf{k}} \delta(\epsilon_{\mathbf{k}} - \epsilon) = \sum_{\mathbf{k}} \delta(\epsilon'_{\mathbf{k}} - \epsilon)$. The ferromagnetic state has higher energy in this case as well.

It is not difficult to go beyond the classical spin approximation to show that there are linearly dispersed spin waves in the antiferromagnetic state. Here the quantum fluctuations are stronger because the classical antiferromagnetic spin state is not an eigenstate of the Hamiltonian. The actual staggered magnetization is smaller due to fluctuations. But it does not change the fact that the antiferromagnetic state has lower energy since the true antiferromagnetic state has even lower energy than the classical state.

The properties of the ferromagnetic state are totally different from those of the antiferromagnetic state. It is not a total surprise that other states have lower energy in the region between the two phases, as found in Ref. [6]. Here we consider two homogeneous states which are natural candidates, the spiral state and the CAF state.

The spiral state was considered as a possible description of doped high T_c systems [14], although few supportive experimental evidences have been found so far. The spiral state is a compromise between the hopping of the holes and the effective superexchange interaction of the electrons. The ferromagnetic and antiferromagnetic phases are just two extreme cases of the spiral phase. The possibility of a spiral phase was considered in the DE model with exchange

interaction in the large Hund coupling limit [15]. It was found that there is a transition from the ferromagnetic phase to the spiral phase near zero doping as a function of the exchange coupling. However, it was not addressed whether the spiral phase exists or not in the simple DE model with arbitrary Hund coupling and without any exchange interaction.

In a spiral state, the Kondo spin is aligned in a certain plane and the angle of the spin is a linear function of its site position vector. For simplicity, we consider the spins in the x - y plane and choose the classical Schwinger-boson operators to be $b_{i\uparrow} = \sqrt{S}e^{-i\mathbf{Q}\cdot\mathbf{R}_i}$ and $b_{i\downarrow} = \sqrt{S}e^{i\mathbf{Q}\cdot\mathbf{R}_i}$. The Hamiltonian is now given by

$$\begin{aligned} \mathcal{H} = & - \sum_{\langle ij \rangle} \left[\cos(\mathbf{Q} \cdot (\mathbf{R}_i - \mathbf{R}_j)) (f_i^\dagger f_j + h_j^\dagger h_i) + i \sin(\mathbf{Q} \cdot (\mathbf{R}_i - \mathbf{R}_j)) (f_i^\dagger h_j - h_j^\dagger f_i) \right] \\ & - \frac{JS}{2} \sum_i (f_i^\dagger f_i - h_i^\dagger h_i). \end{aligned} \quad (4)$$

For symmetry reasons, we consider the \mathbf{Q} -wavevector in $(1, 1, 1)$ direction which is equivalent to all the other $(\pm 1, \pm 1, \pm 1)$ directions. After diagonalizing this Hamiltonian, we obtain two free fermion bands with dispersion given by

$$E_{\mathbf{k}} = \cos(Q_x a) \epsilon_{\mathbf{k}} \pm \sqrt{\frac{J^2 S^2}{4} + \sin(Q_x a)^2 \epsilon_{\mathbf{k}}^2}. \quad (5)$$

The ferromagnetic phase is a special case with $\mathbf{Q} = 0$ and the antiferromagnetic phase is another special case with $Q_x = \pi/2$. The wavevector \mathbf{Q} of the preferred spiral state can be obtained by minimizing the total energy.

In a CAF state, each sublattice has different magnetization directions. The uniform magnetization coexists with the staggered magnetization. The ferromagnetic and antiferromagnetic states are also two special cases of the CAF states. To study the CAF state, we take the z -direction to be the direction of the uniform component and x -direction to be the direction of the staggered component, with the b -values given by $b_{i\uparrow} = b_1$ and $b_{i\downarrow} = (-1)^i b_2$. The Hamiltonian can be easily diagonalized. The fermions form two bands with dispersion given by

$$E_{\mathbf{k}} = \pm \sqrt{\left(\frac{JS}{2}\right)^2 + \epsilon_{\mathbf{k}}^2} + JS_z \epsilon_{\mathbf{k}}, \quad (6)$$

where the uniform magnetization is given by $S_z = (|b_1|^2 - |b_2|^2)/2$.

We compared the energies of different states. The CAF states always have higher energy than the spiral state. In Fig. 1, the energy of the 3D DE model is plotted as a function of hole density. As shown in this figure, the ferromagnetic phase always have the lowest energy when the hole density is above certain value; below this density, the spiral phase has lower energy. At half filling, the antiferromagnetic phase has the lowest energy. However, near half filling, as shown in Fig. 1, the spiral phase is always unstable due to its negative compressibility and it is subject to phase separation. One of the phases in phase separation is the antiferromagnetic phase. Depending on the value of $JS/4dt$, the other phase can be either ferromagnetic phase or the spiral phase.

To determine the phase boundary where phase separation occurs we use in the following method. Let x be the overall hole density of the system and y be the ratio of the volume of the ferromagnetic regions or the spiral regions to the total system volume, the total energy of the system per site is given by

$$E(x, y) = (1 - y)E_A + yE_B\left(\frac{x}{y}\right), \quad (7)$$

where E_A is the energy of the antiferromagnetic phase per site and $E_B(x)$ is the energy of the ferromagnetic or the spiral phase per site at hole density x . Since the energy $E(x, y)$ is at minimum as a function of y , the stability condition $\partial_y E(x, y) = 0$ produces the equation

$$E_A = E_B\left(\frac{x}{y}\right) - \frac{x}{y} E_B'\left(\frac{x}{y}\right). \quad (8)$$

The solution of eq. (8) is given by

$$\frac{x}{y} = x_c, \quad (9)$$

where the constant x_c is the critical hole density of the system since the phase boundary is determined by $y = 1$. The hole density of the spiral regions or ferromagnetic regions x/y is always equal to the critical hole density x_c .

We find that the system separates into the spiral phase and the antiferromagnetic phase when $\frac{JS}{4dt}$ is smaller than certain value. When $\frac{JS}{4dt}$ is bigger than this critical value, the spiral phase disappears completely and the phase separation is between the ferromagnetic phase and the antiferromagnetic phase. In 3D, the critical ratio is about $2/3$; it is about 0.84 in 2D. In both cases, the critical hole density of phase separation boundary vanishes in the limit of $J \rightarrow \infty$ and also in the limit of $J \rightarrow 0$.

The complete 3D and 2D phase diagrams are shown in Fig. 2 and Fig. 3. Overall there are five phases: the antiferromagnetic phase, the ferromagnetic phase, the spiral phase, phase separation between the antiferromagnetic phase and the ferromagnetic phase, and phase separation between the antiferromagnetic phase and the spiral phase. The phase transitions are likely to be second order because both the energy derivative and the sizes of various phase regions are continuous across the phase transition lines. The 3D phase diagram has a tricritical point at $\frac{JS}{4dt} \approx \frac{2}{3}$, $x \approx 0.38$; the tricritical point of 2D phase diagram is located at $\frac{JS}{4dt} \approx 0.84$, $x \approx 0.35$. However, the 3D and 2D phase diagrams has one major difference. In 3D, in the limit $J \rightarrow 0$, the critical density between the ferromagnetic phase and the spiral phase is 0.55; in 2D, it is unity.

In Fig. 3, numerical data from Ref. [6] are also plotted. The agreement is reasonably good considering that the spin fluctuations could quantitatively modify our results and that the finite size effect could affect the numerical results. Although it is beyond the scope of our paper, we expect that the spin fluctuations of the spiral states are described by quadratically dispersed spin waves, similar to the ferromagnetic case. The dispersion should become more linear as doping decreases. It is very unlikely that the spin waves will make any qualitative changes to the phase diagrams in 3D and 2D, although more accurate numerical phase diagrams are also needed to make comparison.

In one dimension however, quantum fluctuations in principle destroy any broken symmetry states. But as found in Ref. [6], phase diagrams of 1D systems are very similar to 2D phase diagrams. It is important to go beyond the classical spin approximation to study 1D systems and the effects of spin fluctuations.

In conclusion, we find that in the large-S limit of the DE model the spiral phase is an intermediate phase between the ferromagnetic phase and the antiferromagnetic phase when the Hund coupling is relatively small. Near half filling, the system subjects to phase separation. The 2D phase diagram that we have found is consistent with the numerical results [6]. Future studies on more sophisticated DE model is needed to relate to CMR systems.

The author would like to thank Sanjoy Sarker, Steven Kivelson and especially Tin-Lun Ho for helpful discussions. The author was supported by the National Science Foundation under Grant No. DMR 0201948 during the stay in University of Washington, and is currently supported by NSFC under Grant No. 10174003 and by SRF for ROCS, SEM.

-
- [1] For introduction, see S. Jin, T. H. Tiefel, M. McCormack, R. A. Fastnacht, and L. H. Chen, *Science* **264**, 413 (1994) and references therein.
 - [2] P. Schiffer, A. P. Ramirez, W. Bao, and S-W. Cheong, *Phys. Rev. Lett.* **75**, 3336 (1995); C.H. Chen and S-W. Cheong, *Phys. Rev. Lett.* **76**, 4042 (1996).
 - [3] C. Zener, *Phys. Rev.* **82**, 403 (1951); P. W. Anderson and H. Hasegawa, *ibid.*, **100**, 675 (1955).
 - [4] K. Kubo and N. Ohata, *J. Phys. Soc. Jpn.* **33**, 21(1972); N. Furukawa, *J. Phys. Soc. Jpn.* **63**, 3214 (1994).
 - [5] P. G. de Gennes, *Phys. Rev.* **118**, 141 (1960).
 - [6] S. Yunoki, J. Hu, A. L. Malvezzi, A. Moreo, N. Furukawa, and E. Dagotto, *Phys. Rev. Lett.* **80**, 845 (1998); E. Dagotto, S. Yunoki, A. L. Malvezzi, A. Moreo, J. Hu, S. Capponi, D. Poilblanc, and N. Furukawa, *Phys. Rev. B* **58**, 6414 (1998).
 - [7] A. Moreo, S. Yunoki, and E. Dagotto, *Science* **283**, 2034 (1999); S. Yunoki and A. Moreo, *Phys. Rev. B* **58**, 6403 (1998); S. Yunoki, A. Moreo, and E. Dagotto, *Phys. Rev. Lett.* **81**, 5612 (1998); H. Yi and J. Yu, *Phys. Rev. B* **58**, 11123 (1998); J. L. Alonso, J. A. Capitán, L. A. Fernández, F. Guinea, and V. Martín-Mayor, *Phys. Rev. B* **64**, 054408 (2001).
 - [8] D. P. Arovas, G. Gómez-Santos, F. Guinea, *Phys. Rev. B* **59**, 13569 (1999).
 - [9] S-Q. Shen and Z. D. Wang, *Phys. Rev. B* **58**, R8877 (1998).
 - [10] E. L. Nagaev, *Phys. Rev. B* **58**, 2415 (1998).
 - [11] N-H. Tong and F-C. Pu, *Phys. Rev. B* **62**, 9425 (2000).
 - [12] A. Chattopadhyay, A. J. Millis, S. Das Sarma, *Phys. Rev. B* **64**, 012416 (2001).
 - [13] V. J. Emery, S. A. Kivelson, and H. Q. Lin, *Phys. Rev. Lett.* **64**, 475 (1990).
 - [14] B.I. Shraiman and E.D. Siggia, *Phys. Rev. Lett.* **62**, 1564 (1989); C. Jayaprakash, H. R. Krishnamurthy, S. Sarker, *Phys. Rev. B* **40**, 2610 (1989).
 - [15] J. Inoue and S. Maekawa, *Phys. Rev. Lett.* **74**, 3407 (1998).
 - [16] S. Sarker, *J. Phys. Cond. Mat.* **8**, L515 (1996); D.P. Arovas and F. Guinea, *Phys. Rev. B* **58**, 9150 (1998).

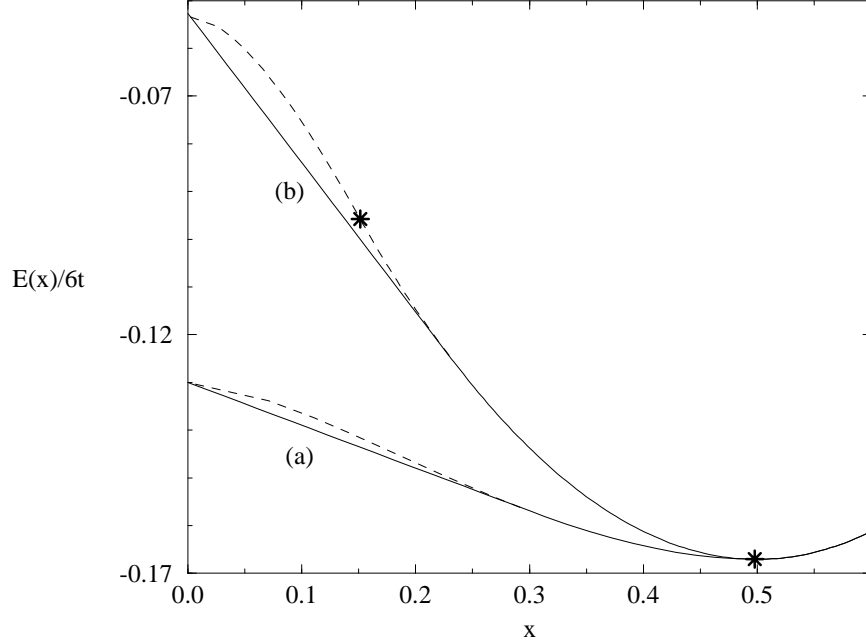


FIG. 1: The energies of the 3D DE model in the large-S limit as a function of hole density x for (a) $JS = 6t$ and (b) $JS = 18t$. $E(x)$ is the total energy per site subtracted by chemical potential $-\frac{1}{2}(1-x)JS$. The solid lines are the lowest energies of the system. In (a), the dotted line is the energy of the spiral state in the phase separation region. The energy of phase separation is given by the straight line below it. The star marks the transition point from the ferromagnetic phase to the spiral phase. In (b), the dotted line is the energy of the spiral state in the phase separation region. The star marks the hypothetical transition point between the spiral phase and the ferromagnetic phase.

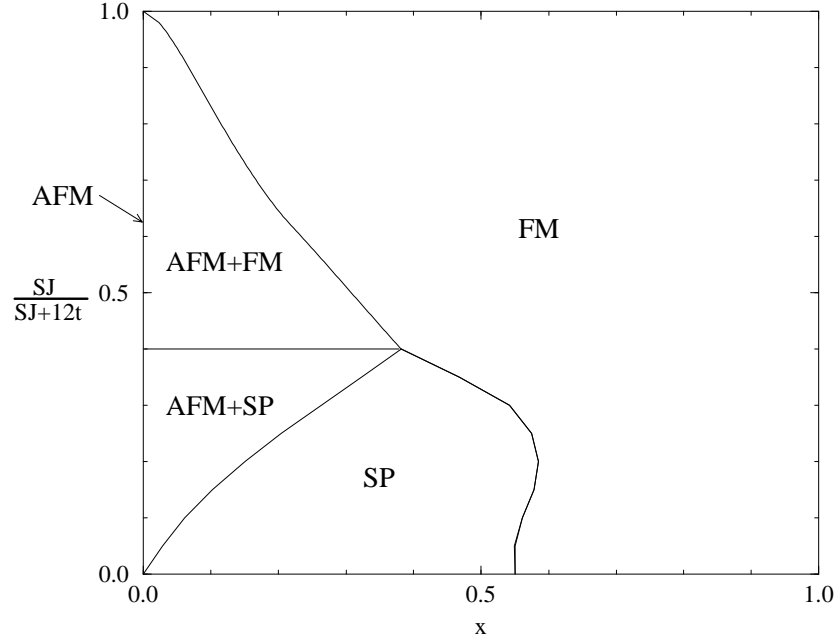


FIG. 2: The zero temperature phase diagram of double exchange model in cubic lattice in the large-S limit. The ferromagnetic phase (FM) exists at high hole density and the antiferromagnetic phase (AFM) exists at half filling. When $\frac{JS}{12t} < \frac{2}{3}$, the spiral phase (SP) appears at low hole density. Phase separation between SP and AFM occurs near zero doping. When $\frac{JS}{12t} > \frac{2}{3}$, phase separation between FM and AFM appears at low doping.

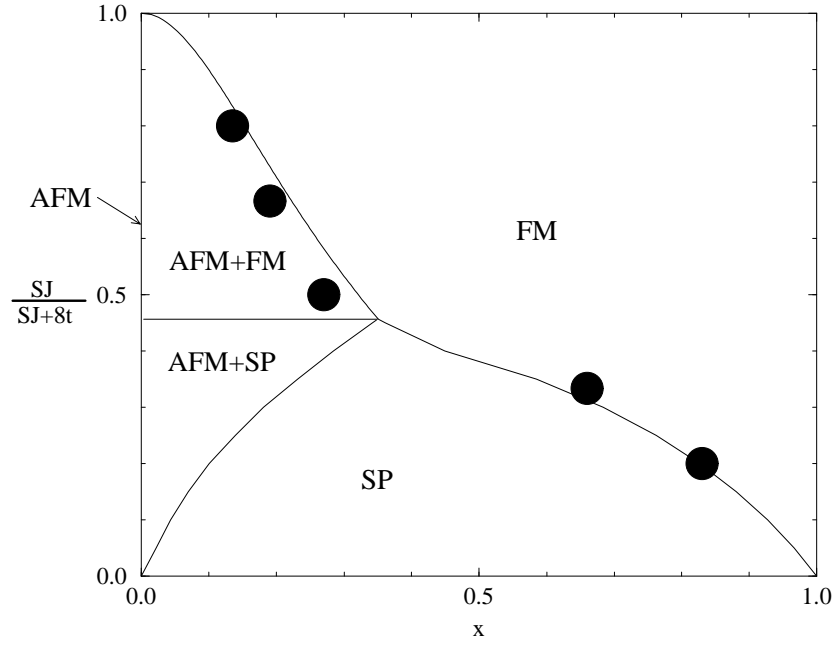


FIG. 3: The zero temperature phase diagram of double exchange model in square lattice in the large-S limit. The black spots are marks of of the phase boundaries taken from Ref.[6].